

# Interaction of Native Cyclodextrins and Their Hydroxypropylated Derivatives with Carbamazepine in Aqueous Solution. Evaluation of Inclusion Complexes and Aggregates Formation

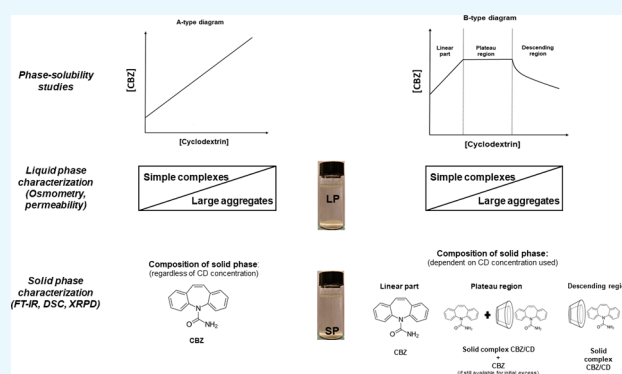
André Rodrigues Sá Couto,<sup>†</sup> Alexey Ryzhakov,<sup>†</sup> Kim Lambertsen Larsen,<sup>‡</sup> and Thorsteinn Loftsson<sup>\*,†</sup>

<sup>†</sup>Faculty of Pharmaceutical Sciences, University of Iceland, Hofsvallagata 53, IS-107 Reykjavik, Iceland

<sup>‡</sup>Department of Chemistry and Bioscience, Aalborg University, Frederik Bajers Vej 7H, DK-9220 Aalborg, Denmark

## Supporting Information

**ABSTRACT:** A detailed comprehensive study on how the formation of soluble and insoluble carbamazepine/cyclodextrins (CBZ/CD) complexes (with consequent changes in the solid-phase composition) depends on the CD structure is not yet available. Moreover, the study of possible influence of this drug on the tendency of CDs and their complexes to self-aggregate is still lacking. Phase-solubility studies demonstrated that CDs and CBZ form a range of soluble ( $A_L$ -type:  $\alpha$ CD,  $\beta$ CD, and hydroxypropylated CDs) and insoluble ( $B_S$ -type:  $\gamma$ CD) complexes depending on CD used. HP $\beta$ CD proved to be the best CD solubilizer for CBZ forming the most stable complex with highest apparent solubility, whereas  $\gamma$ CD was shown to be the best native CD. For the native CDs, CBZ solubilization increases with increasing CD cavity diameter ( $\alpha$ CD  $\ll$   $\beta$ CD <  $\gamma$ CD). Solid phases collected from phase-solubility studies were characterized by Fourier-transformed infrared spectroscopy, differential scanning calorimetry, and X-ray powder diffraction to elucidate their composition and crystalline structure. They provided similar conclusions being overall supportive of phase-solubility, osmolality, and permeation studies results. Solid CBZ was the only detected component for  $A_L$ -type profiles over the CD concentration range studied, whereas precipitation of poorly soluble CBZ/ $\gamma$ CD complexes ( $B_S$ -type) was observed (i.e., at and beyond plateau region). Osmometry and permeation studies were applied to evaluate the effect of CBZ on the aggregate formation and also to elucidate their influence on CD complex solubility and permeation profile. Permeation method was shown to be the most effective method to detect and evaluate aggregate formation in aqueous  $\gamma$ CD and HP $\beta$ CD solutions containing CBZ. CBZ did not affect the HP $\beta$ CD tendency to self-aggregate but CBZ did modify the aggregation behavior of  $\gamma$ CD decreasing the apparent critical aggregation concentration value from 4.2% (w/v) (in pure aqueous  $\gamma$ CD solution) to 2.5% (w/v) (when CBZ was present).



## 1. INTRODUCTION

Carbamazepine (CBZ), 5H-dibenz[b,f]azepine-5-carboxamide, is the most widely used anticonvulsant drug for the treatment of psychomotor epilepsy. Although effective, CBZ constitutes a challenge for pharmaceutical formulators because of its low water solubility (approximately <200  $\mu$ g/mL), slow dissolution rate, and polymorphism.<sup>1–5</sup> Four different anhydrous forms, and a dihydrate has been described in the literature, where polymorph form I and form III are the most frequently encountered.<sup>6–8</sup>

Although the different polymorphic forms of CBZ may exhibit different dissolution rates and bioavailabilities, selection of one polymorphic form over the others in a formulation may not be a viable route for improving the bioavailability of the drug. Other methods are needed to overcome the formulation limitations of CBZ (polymorphism and poor dissolution rate), one of which is the use of cyclodextrins (CD).<sup>9–13</sup> These pharmacopoeial approved excipients are very useful and used

in several commercialized products (pharmaceutical, chemical, food, cosmetic, etc.) because of their safe toxicological profile and ability to form water-soluble complexes.<sup>12,14–18</sup>

In aqueous media, CDs can form inclusion complexes with a lipophilic molecule or part of a larger molecule or through formation of noninclusion complexes.<sup>9,17,19</sup> Solubilization of drugs, through a micelle-like mechanism, may also occur through formation of CD and/or drug/CD complex aggregates.<sup>14,20</sup> This ability of CDs to self-aggregate needs to be controlled by pharmaceutical formulators, as it sometimes needs to be prevented (can cause formulation instability provoking therapeutical and economical losses) but may also be advantageous for creation of novel drug delivery systems because of its simplicity and versatility.<sup>12</sup>

Received: August 15, 2018

Accepted: December 13, 2018

Published: January 16, 2019

Several studies of the interaction between CBZ and  $\alpha$ CD,<sup>21</sup>  $\beta$ CD,<sup>1–3,5,21–23</sup>  $\gamma$ CD,<sup>13</sup> HP $\beta$ CD,<sup>13,19,21,24–26</sup> HE $\beta$ CD,<sup>13</sup> DM $\beta$ CD,<sup>13</sup> SBE $\beta$ CD,<sup>4,27</sup> and HP $\gamma$ CD<sup>13</sup> have already been published. However, a systematic, detailed, and comprehensive study on the dependence of CD type on the formation of soluble and insoluble complexes is not yet available. The majority of the studies mentioned above utilize classic phase-solubility studies to characterize the potential of different CD types to increase the apparent solubility of CBZ by focusing on the increase of CBZ concentration in solution dependent on initial CD concentration. The composition and changes in composition of the solid phase are, as for the majority of studies on drug/CD complexes by phase-solubility experiments, fully ignored. Moreover, changes in the composition of the solid phase with respect to CD concentration as a consequence of possible formation of poorly soluble CD/drug complexes have also not been studied. Furthermore, none of the previous publications on this topic have focused on and described the possible influence of CBZ on the self-aggregation behavior of these CDs and their complexes. The aim of the present study is to provide a better understanding of the interaction of CBZ with a range of relevant CDs (varying cavity sizes:  $\alpha$ CD,  $\beta$ CD, and  $\gamma$ CD; and by comparing native and hydroxypropylated CDs) on the basis of phase-solubility studies including characterization of changes in the composition of the solid phase, changes in the concentration of CD in solution as compared to the initial concentration, and the formation of aggregates. To elucidate the composition and crystalline structure of the solid phases, we have characterized the solid phases obtained from the phase-solubility studies by Fourier transform infrared spectroscopy (FTIR), differential scanning calorimetry (DSC), and X-ray powder diffraction (XRPD), some of which are reported in the [Supporting Information](#). The liquid phases were analyzed using permeation and osmolality methods for the determination of the influences of CBZ on the flux profile and apparent critical aggregation concentration (cac) of the CDs.

## 2. RESULTS AND DISCUSSION

In the first part of this study, we attempt to correlate the type of CBZ/CDs phase-solubility diagrams with the composition of the obtained solid phases and elucidate the importance of CD type on complexation and solubilization of these systems. To get insight into the nature of the solid phase, we have used diverse analytical techniques as previously mentioned. For these tests, A-type phase-solubility profiles were tested at the highest CD concentration used, whereas B-type phase-solubility profiles were at least tested at two concentrations (i.e., before and after the plateau region).

In the second part of this study, we aim to understand and evaluate not only if/how CBZ can affect the flux and apparent tendency of studied CDs to self-aggregate (comparing apparent cac values) when associated in inclusion/non-inclusion complexes but also how the CDs complexes modulate CBZ permeability through a semi-permeable membrane. This novel insight was mainly possible because of the performance of osmometry and permeation studies. Another novelty of this work compared with most publications in this field (where presented graphs and values are based on theoretical CD concentrations) was the use of Corona detector that allowed us to quantify the actual concentration of CDs and drug (simultaneously) present in liquid phases.

**2.1. Phase-Solubility Studies.** Usually the apparent water solubility of drug is enhanced by the formation of drug/CD complexes. To evaluate the interaction between CDs and CBZ, phase-solubility diagrams were made by plotting the concentration of CBZ brought into solution versus the actual (as opposed to added) CD concentration ([Figures 1 and 2](#)).

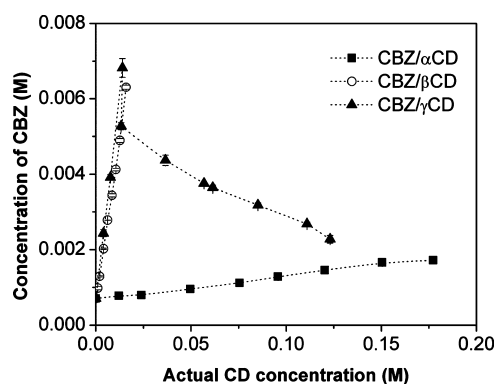


**Figure 1.** Phase-solubility profile describing solubility of CBZ in aqueous  $\alpha$ CD,  $\beta$ CD, and  $\gamma$ CD solutions at 25 °C. Symbols represent mean  $\pm$  SD ( $n = 3$ ).

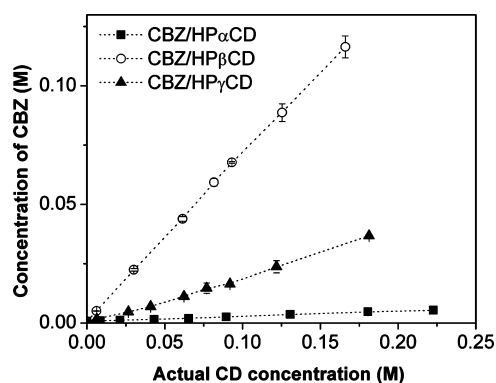


**Figure 2.** Obtained phase-solubility profiles for HP-CDs with CBZ (25 °C). Symbols represent mean  $\pm$  SD ( $n = 3$ ).

Slopes were calculated by plotting all concentration range in case of A-type diagrams or just using the initial linear portion (for B-type diagrams). Using the apparent intrinsic solubility ( $S_0$ ) of CBZ and determined slopes, we were able to determine apparent stability constants ( $K_{1:1}$ ) and the complexation efficiencies (CE). Also, the maximum increase (in percentage) in apparent solubility of CBZ per mM of CD (IS) was calculated ([Table 1](#)).

It has previously been described in the literature that native CDs have low aqueous solubility compared with their hydroxypropylated derivatives and that the native CDs are more prone to self-assembly and aggregate formation. This phenomenon can contribute for the definition of phase-solubility profiles of many drugs.<sup>28,29</sup>

**2.1.1. Native CDs.** Hydroxypropylated CD derivatives (i.e., HP $\alpha$ CD, HP $\beta$ CD, and HP $\gamma$ CD) are obtained by random substitution that transforms the crystalline native CDs into amorphous mixtures of large number of isomers.<sup>31,32</sup> Thus, HP $\alpha$ CD, HP $\beta$ CD, and HP $\gamma$ CD and their complexes are unable to form crystals in aqueous solutions and, because of their enhanced solubility, generally display A<sub>L</sub>-type phase solubility diagrams. On the other hand, native CDs and their complexes

**Table 1. Type of Profile, Apparent Stability Constant ( $K_{1:1}$ ), CE and Maximum Increase (in Percentage) in Apparent Solubility of CBZ per mM of CD (IS) in the Different Aqueous CBZ/CD Complex Solutions at 25 °C<sup>a</sup>**

CD	carbamazepine (CBZ)				
	type <sup>b</sup>	slope	$K_{1:1}$ (M <sup>-1</sup> )	CE	IS (%)
$\alpha$ CD	A <sub>L</sub>	0.006	8.9	0.006	0.97
$\beta$ CD	A <sub>L</sub>	0.348	840.5	0.53	56.4
$\gamma$ CD	B <sub>S</sub>	0.441	1245.1	0.79	69.9
HP $\alpha$ CD	A <sub>L</sub>	0.022	31.4	0.02	3.4
HP $\beta$ CD	A <sub>L</sub>	0.699	3299.5	2.33	110.1
HP $\gamma$ CD	A <sub>L</sub>	0.189	369.0	0.23	31.5

<sup>a</sup>Phase-solubility diagrams built with actual CD concentrations instead of theoretical CD concentrations only showed some differences for the B-type diagrams (i.e., beyond the plateau region). As their initial linear part (i.e., before the plateau region) showed negligible changes, Higuchi–Connors classification could still be used. <sup>b</sup>A<sub>L</sub>: linear phase-solubility diagram and B<sub>S</sub>: phase-solubility diagram with linear initial increase, a plateau and a decreasing terminal solubility.<sup>30</sup>

can form crystalline solid state and, thus, display limited solubility in water that frequently leads to B-type phase-solubility profiles. However, in case of CBZ, only  $\gamma$ CD presented the B<sub>S</sub>-type profile while  $\alpha$ CD and  $\beta$ CD displayed A<sub>L</sub>-type (Table 1). We believe that for  $\beta$ CD, the A-type phase-solubility diagram is only observed because of the poor solubility of  $\beta$ CD (high enough  $\beta$ CD concentrations to observe B<sub>S</sub>-type diagrams are not possible to achieve).

Figure 1 shows the phase-solubility profile for native CDs with CBZ. Combining the analysis of this figure with results of Table 1, it is possible to see that  $\alpha$ CD and CBZ did not have a good interaction although it displayed A<sub>L</sub> phase-solubility profile.  $K_{1:1}$  and CE values (8.9 M<sup>-1</sup> and 0.006, respectively) are extremely small pointing to the fact that  $\alpha$ CD cavity is too small to host/interact with any part of CBZ.

As already mentioned, because of low aqueous solubility,  $\beta$ CD displayed an A<sub>L</sub> phase-solubility profile with CBZ (Figure 1). Apparent solubility of formed complex increased linearly with increasing  $\beta$ CD concentration. Complexation of CBZ by  $\beta$ CD was possible and more effective when compared to  $\alpha$ CD as all parameters described in Table 1 increased significantly.

Generally,  $\gamma$ CD displays B<sub>S</sub>-type profiles with guests and CBZ was not an exception. In Figure 1, a typical B<sub>S</sub>-profile for  $\gamma$ CD with characteristic regions is presented: First, a linear region, where the increase of CD concentration leads to the formation of water-soluble CBZ/ $\gamma$ CD complexes that, consequently, increase CBZ total solubility. Thereafter a plateau region, where the maximum CBZ solubility is achieved, was expected. This region is not apparent from the data obtained. Finally, the descendent part is achieved and it is characterized by the decrease of apparent CBZ solubility due to formation of insoluble CBZ/ $\gamma$ CD complexes. This happens because all the solid CBZ has been brought into solution or precipitated as CD complex and that the increase in  $\gamma$ CD concentration will promote precipitation of the complex.

Overall, all calculated parameters presented in Table 1 (slope,  $K_{1:1}$ , CE, and IS) increased with increasing CD cavity size ( $\alpha$ CD <  $\beta$ CD <  $\gamma$ CD). Concerning the linear part of the phase-solubility diagrams,  $\gamma$ CD registered the highest value for CE and IS of the native CDs showing that this was the native

CD that interacted the strongest (i.e., formed most stable complex) and brought the most CBZ into solution.

All registered slopes were smaller than unity which suggests the formation of simple 1:1 CBZ/native CD complexes in accordance with literature.<sup>3,13,21,22,24</sup>

**2.1.2. Hydroxypropylated Cyclodextrins.** The phase-solubility diagrams obtained for the hydroxypropylated CDs (HP-CDs) also gave straight lines characteristic for A<sub>L</sub>-type profiles (Figure 2).

These modified CDs were capable of solubilizing CBZ and to increase its apparent solubility with increasing CD concentration linearly. Similarly to  $\alpha$ CD, HP $\alpha$ CD was also the least efficient CD of this group to bring CBZ into solution. The smaller cavity size probably hinders the interaction as revealed by the calculated parameters (i.e.,  $K_{1:1}$  = 31.4 M<sup>-1</sup>; CE = 0.022).

On the basis of calculated parameters ( $K_{1:1}$ , CE, and IS), it is possible to see that HP $\beta$ CD was overall the best CD tested because it formed the most stable complex and resulted in the largest increase in CBZ solubility (Figure 2 and Table 1).

The observed slope values were smaller than unity, which is an indication that complex formation follows a simple 1:1 stoichiometry also in the case of CBZ/HP-CD systems. Several authors using phase-solubility studies in combination with other analytical methods (e.g., FTIR, DSC, and XRPD) have also reported similar data. They also found evidence of simple inclusion complex formation (1:1 complexes) after interaction of CBZ with HP $\beta$ CD<sup>13,19,21,24–26,33</sup> and HP $\gamma$ CD,<sup>13,33</sup> although always presenting smaller apparent  $K_{1:1}$  values compared with those presented here. However, these discrepancies may be due to the use of a different type of HP $\beta$ CD compared with the other studies (e.g., different manufactures of HP $\beta$ CD producing products with varying DS).

Contrary to the native CDs, analysis of the slope  $K_{1:1}$ , CE, IS for CBZ/HP-CDs (Table 1) does not suggest direct influence of CD central cavity diameter on the increase of CBZ solubilization/complexation.

## 2.2. Characterization of Solid-Phase Compositions.

The composition of solid phases resulting from the phase-solubility studies (Section 2.1) was determined by FTIR spectroscopy, DSC, and XRPD.

All techniques provided similar conclusions (see the Supporting Information), and results were supportive of phase-solubility experiments. The composition of the solid phase can be predicted from the phase-solubility diagram type and possibly by CD aggregation process (Table 2). This basically originates from the inherent ability of native CD to

**Table 2. Variation of Solid-Phase Composition with Phase-Solubility Type Profile and CD Concentration**

phase-solubility profile	solid phase's composition
A-type	highly soluble complexes remaining in solution. only excess of pure drug can be detected in solid phase.
B-type	content of solid phase will vary with CD concentration and surplus amount of model drug. region before plateau $\gg$ only pure model drug. plateau region $\gg$ a mixture of pure drug and insoluble complexes will be found. post plateau $\gg$ will mostly consist on solid complex, although it is not possible to exclude the presence of pure drug (depending on the initial excess of drug added and availability of CD in liquid phase at that stage).



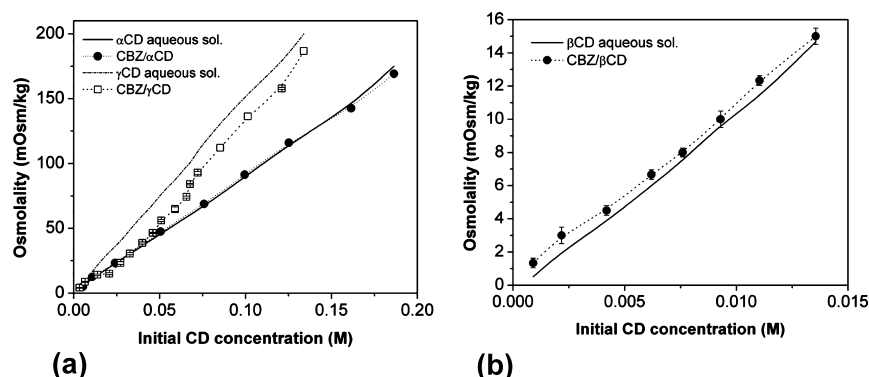


**Figure 3.** (a) Changes of total osmolality for the prepared CBZ/ $\alpha$ CD and CBZ/ $\gamma$ CD systems during phase-solubility experiments (25 °C). (b) Changes of total osmolality for the CBZ/ $\beta$ CD systems during phase-solubility experiments (25 °C). Symbols represent mean  $\pm$  SD ( $n = 3$ ).

form insoluble complexes (resulting in B-type phase solubility diagrams), a trait not found for typical randomly modified CD's (e.g., commercially available hydroxypropyl derivatives). Here, their inability to form insoluble complexes most often results in A-type diagrams in the concentration ranges studied.

**2.3. Osmolality Measurements.** Osmometry is a colligative property that indicates the number of all osmotically active molecules dissolved in the solvent and in our previous research proved to be quite useful to detect native CDs aggregates.<sup>34</sup>

In an attempt to detect/quantify CBZ/CD inclusion complexes aggregates and also tracing possible changes in the apparent solubility of the CD complexes as a consequence of interaction with soluble CBZ, the osmometry method was applied to liquid phases from the phase-solubility experiment after careful separation of the liquid and solid phases.

The osmolality of freshly prepared CD aqueous solutions (represented by lines) and CD solutions saturated with CBZ (represented by symbols with lines) were plotted against CD concentrations. We expect that total osmolality will remain constant or become slightly higher in case of the formation of soluble complexes. Total osmolality will be equal to osmolality of CD plus the one obtained from increased apparent solubility of CBZ (as CD is present in higher amount, usually this possible osmolality increase is only visible for  $\beta$ CD complexes). On the other hand, we will observe a decrease in total osmolality in the case of systems that displayed phase-solubility B-type, as from some region (beyond plateau) precipitation of solid complex will decrease the particle concentration in the solution.

**2.3.1. Native CDs.** Different trends in osmolality behavior were registered for native CDs after interaction with CBZ, depending on the sample phase-solubility type (Figure 3).

For CBZ/ $\alpha$ CD liquid phases, almost no changes were observed in osmolality from samples saturated with CBZ (Figure 3a). This is in accordance with phase-solubility results as the presented osmolality plot is typical from A<sub>L</sub>-type profiles.

In the case of CBZ/ $\beta$ CD, the presence of CBZ promotes a small constant increase of the osmolality of the CD solutions throughout the concentration range (Figure 3b).

Commonly, samples containing  $\gamma$ CD show negative deviations of osmolality from stock solutions trend, caused by a decrease in particle concentration due to the precipitation of poorly soluble CBZ/ $\gamma$ CD complexes at a certain CD concentration (Figure 3a). The B<sub>S</sub>-type profile nature of this system justifies the appearance of CBZ/ $\gamma$ CD osmolality

graphic that can be divided into three characteristic regions. As saturation concentration for the complex is achieved with relatively low  $\gamma$ CD concentrations, the two first regions are relatively short. First, we observe the linear region (until  $\sim 0.006$  M) where the CBZ/ $\gamma$ CD complex contributes to the increase of system osmolality because the osmolality of the solution containing both CBZ and  $\gamma$ CD is higher than that observed for the  $\gamma$ CD stock solution alone. This effect will continue until the crossing point with the CD curve (second region represented by a small plateau from  $\sim 0.006$  to 0.014 M) where the poorly soluble CBZ/ $\gamma$ CD complex starts to form and overall osmolality will remain almost unalterable. Then, we enter on the last region for this system (beyond plateau region, from  $\sim 0.014$  M), where precipitation of poorly soluble complex stops because of unavailability of solid CBZ, and adding more  $\gamma$ CD will only increase the amount of free  $\gamma$ CD in solution. Because of this, the total osmolality of the system starts to increase again, however, never reaching  $\gamma$ CD stock solution values (dot line in Figure 3a).

**2.3.2. Hydroxypropylated Cyclodextrins.** Similarly, to the CBZ/ $\alpha$ CD and CBZ/ $\beta$ CD systems (A<sub>L</sub>-type), also the saturation of HP-CDs with CBZ did not provide any significant change on system total osmolality (Figure 4). It is typical for A-type profiles that throughout the CD concentration range, the amount of osmotically active particles remains the same or slightly higher in comparison with the initial CD stock solution. The described behavior observed in Figure 4 excludes the possibility of formation and precipitation of CBZ/HP-CDs inclusion complexes.

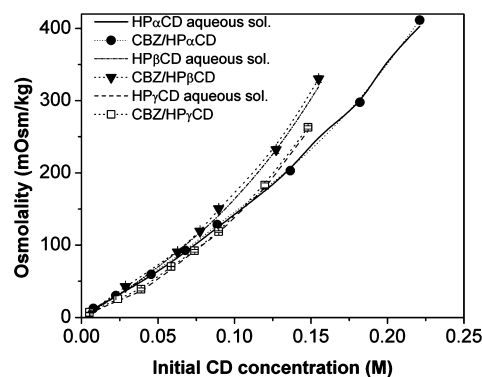


**Figure 4.** Total osmolality changes for of the prepared CBZ/HP-CD systems during phase-solubility experiments (25 °C). Symbols represent mean  $\pm$  SD ( $n = 3$ ).

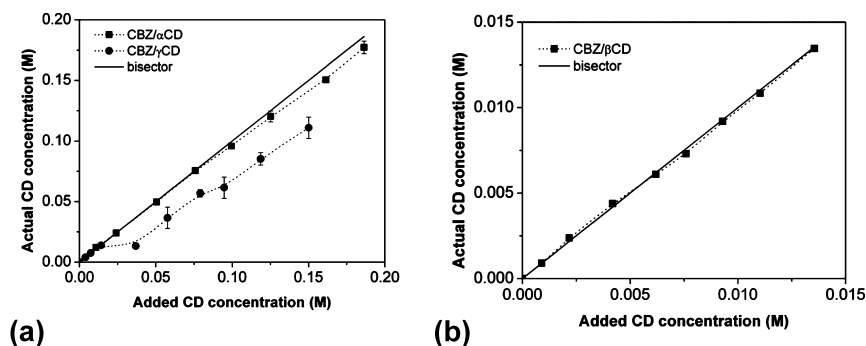


**Figure 5.** Illustration of  $\alpha$ - and  $\gamma$ CD (a) and  $\beta$ CD (b) solubility in the prepared CBZ/CD systems. Symbols represent mean  $\pm$  SD ( $n = 3$ ).

Altogether, these observations corroborate phase-solubility results for HP-CDs, where they displayed  $A_L$ -type.

Osmometry proved to be a simple and reliable method to determine phase-solubility profiles of the studied systems.

However and contrary to what we described for native CD aqueous solutions,<sup>34</sup> this method was not capable of detecting CD aggregate formation and determine the possible modulation of these inclusion complexes on the self-assembly process of the CDs. The precipitation of inclusion complexes (that occurs for B-type profiles) and the increase of the systems osmolality due to increase of CBZ concentration makes it difficult to interpret deviations that occur in total osmolality of these systems (e.g., osmolality can decrease due to precipitation of components, presence of aggregates, etc.).

**2.4. Solubility of Native and HP Derivatives in the CBZ Media.** To find a plausible justification for the osmolality depression observed in previous chapter, the possible effect of CBZ on CD complexes solubility was accessed. Graphical representations of added CD concentration against actual CD concentration (CD concentration in liquid phase after equilibrium) during phase-solubility studies are provided in Figures 5 and 6. Bisectors (described by solid lines) representing the theoretical situation where added CD concentration equals that in solution were also included in the figures.

For CBZ/ $\alpha$ CD and CBZ/ $\beta$ CD, no significant difference is observed between added  $\alpha$ CD/ $\beta$ CD concentration and the concentration at the end of experiment (Figure 5).

A different behavior was observed for  $\gamma$ CD where no changes in added and actual CD concentration are observed

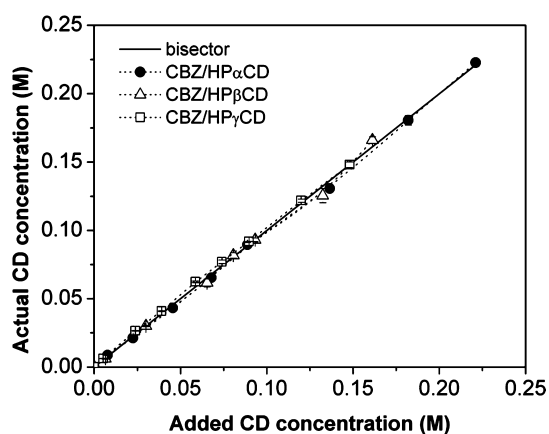
initially in the linear region diverting from the bisector after approximately 0.014 M  $\gamma$ CD (Figure 5a). After saturation concentration of CBZ/ $\gamma$ CD inclusion complex is achieved (matching with the point of diversion from bisector), the plateau region is reached and precipitation of the complex (consequently also CD) takes place. When solid CBZ is no longer available in the system, the additional amount of CD provided will lead to its accumulation in liquid phase. This phenomenon explains the increase in actual  $\gamma$ CD concentration visible in Figure 5a after the plateau region (from  $\sim$ 0.037 M).

Figure 6 shows that CBZ, as expected by  $A_L$  phase-solubility profile, did not have any influence and changed the solubility of HP-CDs over the phase-solubility experiment. This can be explained by the formation of complexes with high aqueous solubility.

**2.5. Permeation Studies.** For these experiments, two representative CBZ/CD systems were selected: native  $\gamma$ CD and HP $\beta$ CD. These represent two of the most promising candidates for formulation of CBZ as they display the highest CE, apparent  $K_{1:1}$  and IS of the studied CDs. Furthermore, they represent two distinctly different phase-solubility profiles ( $B_S$  and  $A_L$ -type, respectively) and are used in the pharmaceutical field. Thus, it is important to achieve more knowledge on the possible influence that guests and inclusion complexes can have on the self-assembly behavior of these CDs. Knowing more about how guests with different physicochemical properties can modulate the solubility and aggregation process of CDs complexes, we can try to disclose driving factors that can promote or prevent the formation of these structures.

This fits in one of the goals we set for this work, the detection and quantification of CD aggregation in the selected systems (through apparent  $cac$  values). From permeation studies, the apparent  $cac$  cannot be defined as the concentration where CDs start to assemble in larger structures (CD aggregates) but rather the concentration at which the size starts to be a hindering factor for free flow of CDs through the membrane (i.e., the aggregates size becomes greater than the molecular weight-cutoff (MWCO) pore size of the membrane tested and the  $cac$  determined is thus dependent on the choice of MWCO of the membrane).

**2.5.1. Hydroxypropylated  $\beta$ CD.** The potential effect of CBZ on HP $\beta$ CD aggregation behavior was estimated through Franz diffusion cell permeability studies using liquid phases from phase-solubility studies. For this group of experiments, 3.5–5 kDa membrane was used and the flux of HP $\beta$ CD from CBZ/HP $\beta$ CD systems was determined. Afterward, the flux values were plotted versus HP $\beta$ CD concentration and a tangent line



**Figure 6.** Illustration of HP-CDs solubility in the prepared CBZ/HP-CD systems. Symbols represent mean  $\pm$  SD ( $n = 3$ ).

to the flux curve was drawn to determine the concentration point from where the flux curve started to divert from linearity. This estimated value corresponds to the apparent cac value for this MWCO pore size membrane.

Sink conditions<sup>35</sup> were fulfilled for this set of experiments (both HP $\beta$ CD and  $\gamma$ CD) as donor phases did not register significant volume changes (were always less than 0.1 mL), and CD concentration in the end of permeability experiments (donor phase) was always higher than 90% of initial concentration.

In Figure 7, it is possible to observe the flux curves for HP $\beta$ CD aqueous solutions (filled squares) and for HP $\beta$ CD

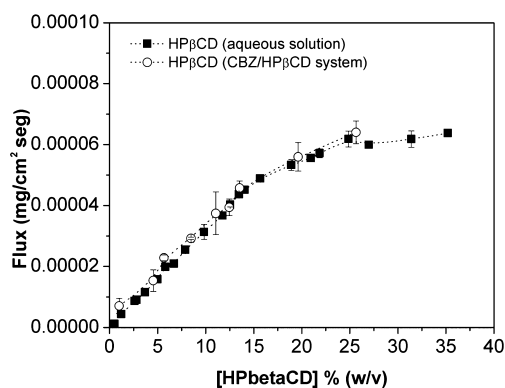


**Figure 7.** Flux profile of HP $\beta$ CD from HP $\beta$ CD aqueous solution (filled squares) and CBZ/HP $\beta$ CD liquid phases (empty circles) through 3.5–5 kDa MWCO semipermeable membrane.

from CBZ/HP $\beta$ CD liquid phases (open circles). The flux behavior of HP $\beta$ CD aqueous solutions was previously studied by our group.<sup>36</sup> Apparent cac value for this system with 3.5–5 kDa MWCO membrane (the same as for the present study) was determined to be 11.8% (w/v). This means that until the apparent cac value HP $\beta$ CD and any formed aggregates permeated freely through the membrane to the receptor phase because they did not have a particle size hindering their diffusion through the membrane pores. Knowing that the molecular weight of HP $\beta$ CD is approximately 1.36 kDa, we could estimate from the apparent cac that the aggregates consisted of approximately 3–4 HP $\beta$ CD monomers at cac.

It is understandable from Figure 7 that no significant difference could be found between HP $\beta$ CD flux curves from HP $\beta$ CD solutions and HP $\beta$ CD from CBZ/HP $\beta$ CD. Apparent cac values (for 3.5–5 kDa) for the CBZ/HP $\beta$ CD systems was estimated to  $\sim$ 11.6% (w/v) which is similar to the one found for pure HP $\beta$ CD solutions. The presence of CBZ did not affect or promote the formation of HP $\beta$ CD aggregates with larger sizes than the one that are naturally formed in HP $\beta$ CD aqueous solutions. Altogether, these results suggest that CBZ did not affect the self-assembly process of HP $\beta$ CD.

**2.5.2. Native  $\gamma$ CD.** Similar to what is described above, the flux curve of  $\gamma$ CD from CBZ/ $\gamma$ CD liquid phases was plotted against actual  $\gamma$ CD concentration and compared with the flux curve from  $\gamma$ CD aqueous solution (Figure 8). The apparent cac value (3.5–5 kDa MWCO) for both systems was calculated and used to study the possible effect of CBZ on natural aggregation of  $\gamma$ CD.

Small but significant differences are noticeable when the flux curve for  $\gamma$ CD in aqueous solution (filled squares) is compared with the one from  $\gamma$ CD from CBZ/ $\gamma$ CD samples (Figure 8).

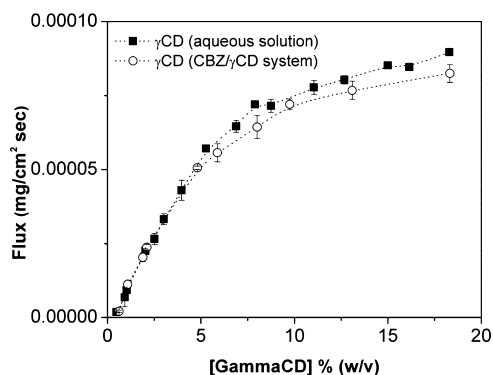


**Figure 8.** Flux profile of  $\gamma$ CD in aqueous  $\gamma$ CD solution (filled squares) and  $\gamma$ CD from CBZ/ $\gamma$ CD liquid phases (empty circles) through 3.5–5 kDa MWCO semipermeable membrane.

$\gamma$ CD flux in aqueous solution increased linearly until a concentration of 4.2% (w/v) (apparent cac value for 3.5–5 kDa) after which a negative deviation probably due to the formation of aggregates and increased in size of aggregates is observed. Beyond this,  $\gamma$ CD concentration aggregates are most likely assembled in sizes larger than the membrane pore size selected for this study, hindering the free flux of  $\gamma$ CD from donor to receptor phase. We can estimate that after 4.2% (w/v)  $\gamma$ CD (MW 1297 Da) solutions, we have aggregated populations of trimers and/or tetramers.

Regarding  $\gamma$ CD from CBZ/ $\gamma$ CD system, we can observe that flux values after a certain  $\gamma$ CD concentration significantly dropped in comparison to  $\gamma$ CD in aqueous solution. This observation was supported by a decrease in the apparent cac value which was estimated to 2.5% (w/v). Until this value, aggregates of  $\gamma$ CD and CBZ/ $\gamma$ CD complexes could be present in the solution with a maximum size of dimers or trimers which are not large enough to make size a permeation limiting factor. After 2.5% (w/v) of  $\gamma$ CD, the flux deviated from linearity as CBZ started to promote the formation of larger structures with sizes larger (more than 3 monomers) than the membrane pore size used in this study (3.5–5 kDa).

The CBZ/ $\gamma$ CD system displayed a B<sub>S</sub>-type diagram in the phase-solubility studies, and it is interesting to note the apparent cac value (for 3.5–5 kDa) and the  $\gamma$ CD concentration at which highest solubility of CBZ/ $\gamma$ CD complex coincides. This suggests that the B<sub>S</sub>-type profile and decrease in apparent CBZ solubility after the plateau region might be related to the aggregate formation of the complex that starts to precipitate out of solution as solid crystalline complexes after this concentration have been reached.

All the collected data strongly suggest that CBZ had an influence on the promotion of  $\gamma$ CD aggregates formation. Similar results were reported in previous publication where indomethacin<sup>37</sup> and parabens<sup>15</sup> proved to influence  $\gamma$ CD aggregation and modulate its permeation profile.

**2.5.3. Influence of HP $\beta$ CD and  $\gamma$ CD on Permeation Behavior of CBZ.** In previous chapters (2.5.1 and 2.5.2), we described the influence of CBZ on the permeability and aggregation profile of HP $\beta$ CD and  $\gamma$ CD complexes. In the present one, we want to investigate the opposite effect, that is, how these two CDs may affect the permeability of CBZ.

Both CDs were capable of forming inclusion complexes with CBZ and thus capable to increase CBZ flux when compared with CBZ alone (in aqueous solution). Figure 9 exemplifies the CBZ flux variation for CBZ/HP $\beta$ CD samples (Figure 9a) and

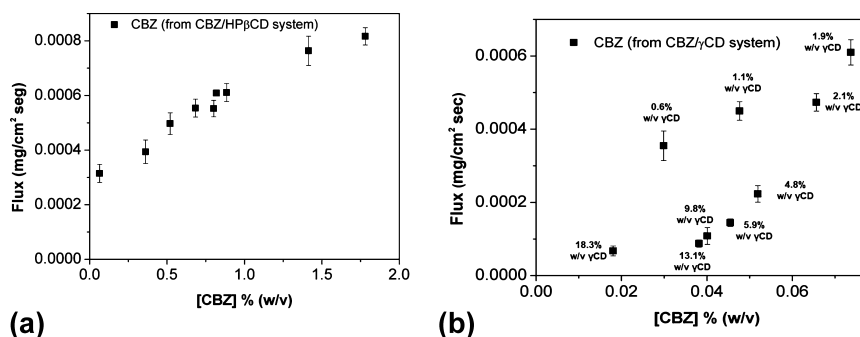


**Figure 9.** Flux profile of CBZ from CBZ/HP $\beta$ CD liquid phases (a) and of CBZ from CBZ/ $\gamma$ CD liquid phases (b) through 3.5–5 kDa MWCO semipermeable membrane.

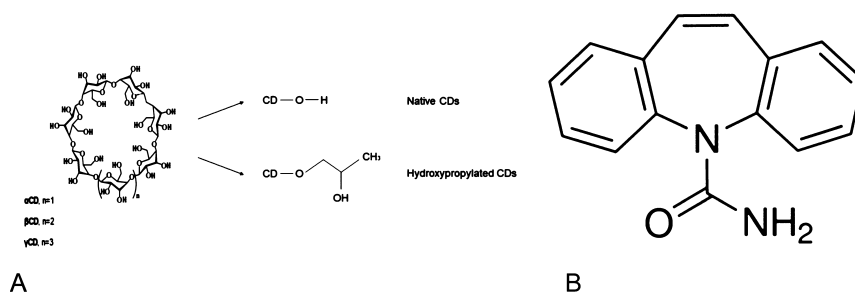


**Figure 10.** Schematic representation of native and hydroxypropylated CDs (A) and CBZ (B). Adapted from ref 39.

for CBZ/ $\gamma$ CD samples (Figure 9b) versus its respective measured CBZ concentration.

Previously, we proved using permeation data that CBZ was not able to modify the natural HP $\beta$ CD permeation profile and to promote any influence over HP $\beta$ CD aggregation. Through evaluation of Figure 9a, we can see a linear increase of CBZ flux with CBZ concentration (following Fick's first law) promoted by the CBZ/HP $\beta$ CD compared with CBZ SE. HP $\beta$ CD is able to increase and facilitate the flux of CBZ molecules from donor to receptor chamber (higher amount of CBZ/HP $\beta$ CD complexes led to increase of CBZ apparent solubility).

Contrarily, CBZ flux from complexed CBZ/ $\gamma$ CD did not present a linear relation with  $\gamma$ CD concentration (Figure 9b). Also, here a possible correlation of phase-solubility type profile ( $B_s$ -type) with the CBZ flux profile (from CBZ/ $\gamma$ CD system) can be used to explain the peculiar shape presented. This flux curve starts with two points with relatively high flux values ( $0.03\%/3.5 \times 10^{-4}$  and  $0.048\%/4.5 \times 10^{-4}$ ) corresponding to the linear part of phase-solubility experiment for this system. The presence of increasing amount of soluble CBZ/ $\gamma$ CD inclusion complexes with  $\gamma$ CD concentration justifies the increase of CBZ apparent water solubility, as well as the observed flux linear increase. However, it stops as soon as saturation concentration of complex is achieved. This point is depicted in Figure 9b as the one presenting simultaneously highest flux and also highest CBZ concentration ( $0.073\%/6.1 \times 10^{-4}$ ).

Afterward a region where CBZ concentration decreases (due to the precipitation of CBZ/ $\gamma$ CD complexes) and simultaneously the flux (increasing presence of  $\gamma$ CD aggregates) with increasing actual  $\gamma$ CD concentration can be observed. The points analyzed corresponded already to plateau region and beyond. We know that  $\gamma$ CD concentration in solution is stable along plateau part and slowly starts to increase after it (the amount of available  $\gamma$ CD in the liquid phase at this stage will

depend on the solid CBZ added at the beginning of experiment). If  $\gamma$ CD would not affect permeability of CBZ (other than facilitate it by increasing its solubility), we should observe an overlapping with previously described CBZ flux points. This means that samples with same CBZ concentration should present same flux values, however, that did not happen because those samples have also different amounts of  $\gamma$ CD which probably explains the peculiar shape flux curve registered.

From the analysis of these results, it is possible to suggest that when the  $\gamma$ CD concentration is increased in solution, more and larger aggregates were formed. These superstructures might be the involved on the precipitation of inclusion complexes and by a decrease of CBZ in liquid phase as a consequence. Their presence in the donor phase might hamper the diffusion of matter from donor to receptor phase leading to the marked drop of CBZ flux shown in Figure 9b.

Our finding that formulations based on inclusion complexes of CBZ/ $\gamma$ CD providing similar concentrations of CBZ (but using different amounts of  $\gamma$ CD) can be produced with different permeability capacities can be an advantage to the pharmaceutical research field. It might be a useful tool especially for ocular or dermal delivery as different types of drug delivery systems can be produced just by using different concentrations of  $\gamma$ CD (or other native CDs) in the formulation (Figure 10).

We can hypothesize that small amounts of  $\gamma$ CD (until plateau region) will allow the production of formulations with fast permeation of components (mainly constitutes by monomers and small aggregates). On the other hand, formulating with higher  $\gamma$ CD concentrations (over plateau region and beyond),  $\gamma$ CD and CBZ/ $\gamma$ CD complex aggregates with larger size and in higher number are formed. The inclusion complex permeability will be slowed down and, consequently, sustained-permeation delivery systems can be produced.



### 3. CONCLUSIONS

Several interesting conclusions could be made from this experimental work. The phase-solubility data could be fitted to a model based on simple 1:1 complex formation suggesting, as previously presented by other authors, that CBZ formed 1:1 complexes with all tested CDs. This does not prove that 1:1 complexes are formed and are responsible for the appearance (linearity) of the phase-solubility curves. It only signifies that the data can be fitted to a model for complex formation based on a simple 1:1 stoichiometry. The lowest apparent solubility increase was obtained for  $\alpha$ CD which almost did not interact with CBZ because of small cavity size (although it displayed  $A_L$ -type), and for  $\gamma$ CD which formed complexes with limited water solubility ( $B_S$ -type), CD cavity size of the native CDs showed to be an important factor for the better solubilization of the drug, increasing with increasing diameter ( $\alpha$ CD  $\ll$   $\beta$ CD  $<$   $\gamma$ CD).

Expectedly, hydroxypropylated CD derivatives also displayed  $A_L$ -type. Because of the larger applicable range of CD concentrations, the solubility enhancement achieved for CBZ can reach higher values than that of their correspondent parent CDs.

HP $\beta$ CD was the best solubilizer agent for CBZ forming the complexes with highest solubility and was most stable ( $K_{1:1} = 3296.3 \text{ M}^{-1}$  and CE = 2.3).  $\gamma$ CD proved to be the best option from native CDs to solubilize CBZ ( $K_{1:1} = 928.9 \text{ M}^{-1}$ ; CE = 0.66 and IS = 69.9%/mM).

Overall the solid-state characterization techniques, as well as osmometry data, provided similar conclusions and were supportive of liquid phase results (phase-solubility, osmolality, and permeation studies). However, in this study, osmometry was not capable to reveal any possible influences of CBZ and its complexes on the aggregation behavior of the CDs (and consequently to determine apparent *cac* values). Nevertheless, osmometry is a fast and reliable method to corroborate or determine phase-solubility profiles.

Permeation studies have shown to be an extremely useful tool to study aggregation and permitted the calculation of apparent *cac* values for both HP $\beta$ CD and  $\gamma$ CD systems.

CBZ did not affect or promote the self-assembly process of HP $\beta$ CD contrary to  $\gamma$ CD where CBZ had a clear influence on the formation of its aggregates.

HP $\beta$ CD had a clear influence on the CBZ flux, increasing linearly with CBZ concentration due to the increase of complexes formed facilitating permeation of CBZ through the membrane. For  $\gamma$ CD, aggregates significantly changed the flux of CBZ through the semipermeable membranes because samples with similar CBZ concentration but with different concentrations of  $\gamma$ CD present completely different permeation abilities as opposed to overlapping of flux curves (more and larger aggregates were formed when  $\gamma$ CD concentration increased yielding lower permeability and consequently lower overall flux).

### 4. MATERIALS AND METHODS

**4.1. Materials.** The native CDs ( $\alpha$ CD,  $\beta$ CD, and  $\gamma$ CD) as well as 2-hydroxypropyl- $\beta$ CD (HP $\beta$ CD) DS 4.2 (MW 1380) were kindly provided by Janssen Pharmaceutica (Beerse, Belgium). 2-Hydroxypropyl- $\alpha$ CD (HP $\alpha$ CD) with degree of substitution 3.6 (MW 1180) and 2-hydroxypropyl- $\gamma$ CD (HP $\gamma$ CD) DS 4.2 (MW 1540) were purchased from Wacker Chemie (Burghausen, Germany). CBZ was also kindly

provided by Janssen Pharmaceutica (Beerse, Belgium). The solvent used for analysis (acetonitrile) was of high-performance liquid chromatography (HPLC) grade and obtained from Sigma-Aldrich (St. Louis, Missouri, USA). Milli-Q water (Millipore, Billerica, MA) was used to prepare CD solutions and mobile phases.

**4.2. CD Solutions Preparation.** Different aqueous CDs stock solutions (taking into account the intrinsic solubility of CD being tested) were prepared. To promote faster dissolution of the CDs, sonication at elevated temperature was used (60 °C/60 min) after which solutions were allowed to cool to room temperature. The test solutions were then prepared by dilution of these stock solutions. The CD concentration range depended on the specific CD.

**4.3. Quantitative Determination of CD/CBZ.** A reverse-phase ultra-HPLC (UHPLC) system from Dionex Softron GmbH (Germering, Germany) was used for the simultaneous determination of CBZ and CDs. The Ultimate 3000 series consisted of a LPG-3400SD pump with a built-in degasser, a WPS-3000 autosampler, a TCC-3100 column compartment, and a Corona ultra RS detector. Phenomenex Kinetex C18 150  $\times$  4.60 mm 5  $\mu$ m column with a matching HPLC Security Guard (Phenomenex, Cheshire, UK) was used. Acetonitrile and water (50:50) were the components of mobile phase. The flow rate was set to 1.0 mL/min, and temperature of the column was set to 30 °C. The injection volume was 10  $\mu$ L. Chromatograms were evaluated using ChromeleonR version 7.2 SR4 (ThermoFisher Scientific, MA, USA).

**4.4. Phase-Solubility Experiments.** Phase-solubility profiles for the CBZ/CD systems were achieved using the isothermal saturation method. Solid CBZ was added in excess amount (that assure the formation of solid phase in equilibrium stage) to each vial together with 3 mL of CD solution of given concentration. This methodology was used for all six CDs tested and was performed in triplicate.

The formed suspensions were kept at 25 °C under constant stirring. After reaching equilibrium (48 h), the mixture was centrifuged for 10 min/3000 rpm using Rotina 35R (Hettich Zentrifugen, Germany). Liquid phases were filtered through a 0.45  $\mu$ m Phenex-RC filter (Phenomenex, Cheshire, UK) and then diluted with Milli-Q water prior to UHPLC analysis. Solid phases were collected and dried in an oven at 35 °C for two days.

The Higuchi and Connors<sup>30</sup> method was used to classify the phase-solubility profiles. The apparent stability constant ( $K_{1:1}$ , eq 1) and the CE (eq 2) were determined from the slope of the linear phase-solubility diagrams plots of the total drug solubility ( $[D_t]$ ) versus total concentration of CD in liquid phase ( $[CD_{liq}]$ ) in moles per liter<sup>26</sup>

$$K_{1:1} = \frac{\text{slope}}{D_0(1 - \text{slope})} \quad (1)$$

$$\text{CE} = \frac{\text{slope}}{1 - \text{slope}} = \frac{[D_t]}{[CD_{liq}]} = K_{1:1} \times S_0 \quad (2)$$

where  $S_0$  is the intrinsic solubility of the CBZ.

The maximum increase (in percentage) in apparent solubility of CBZ per mM of CD (increase in solubility, IS) for each CBZ/CD system was determined as follows (eq 3)

$$\text{IS} = \frac{[CBZ_{\max}] - [CBZS_0]}{[CBZS_0] \times [CD_{\max}]} \times 100 \quad (3)$$



where  $CBZ_{max}$  corresponds to highest solubility of complex and  $CD_{max}$  corresponds to the actual concentration of CD needed to achieve it (measured in the liquid phase at equilibrium). This value was calculated and is valid for linear part of phase-solubility diagrams.

**4.5. Osmolality Measurements.** Osmolality measurements were used to evaluate the aggregation behavior of the CBZ/CD systems. To determine the osmolality of liquid phases, a freezing point osmometer OSMOMAT 30 (Gonotec GmbH, Germany) was used. Calibration was performed with three points: Milli-Q water and by saline standard of 300 or 400 mOsmol/kg NaCl/H<sub>2</sub>O (KNAUER, Germany) depending on concentration range of analyzed samples. For this procedure, only 50  $\mu$ L of the sample was required. Samples were measured immediately after filtration of liquid phases to avoid possible precipitation of components during storage.

**4.6. Permeation Studies.** Unjacketed Franz diffusion cells with diffusion area of 1.77 cm<sup>2</sup> (SES GmbH—Analyse systeme, Germany) were used to determine the possible influence of CBZ on  $\gamma$ CD and HP $\beta$ CD apparent cac values and the effect of these CDs on the capability of CBZ to penetrate semipermeable membranes.

12 mL of Milli-Q autoclaved water (to remove dissolved air) were used as receptor phase, while the donor phase consisted in 2 mL of different liquid phases (from phase-solubility experiments). In between the two compartments, a 3.5–5 kDa MWCO semipermeable cellulose ester membrane (Biotech CE, Spectrum Europe, Breda, NL) was placed. All permeability experiments were carried out at room temperature under continuous magnetic stirring (300 rpm) of receptor phase (donor phase was unstirred).

Sampling was initiated after 1 h for  $\gamma$ CD and 0.25 h for HP $\beta$ CD after which the amount of CBZ diffused into the receptor phase was above the quantification limit. Samples were withdrawn every 15 min hereafter at determined time points: 60–120 min for  $\gamma$ CD and from 15 to 75 min for HP $\beta$ CD, 150  $\mu$ L of sample was collected from the receptor phase and immediately replaced by equal volume of Milli-Q water. UHPLC was used to simultaneously quantify CD and CBZ. Steady-state flux ( $J$ ) of the CBZ/CD was calculated from the slope ( $dq/dt$ ) of the linear regression relationship between time ( $t$ ) and the amount of CBZ and CD in receptor phase (eq 4)

$$J = \frac{dq/dt}{A} = P_{app} \cdot C_d \quad (4)$$

where  $A$  is the diffusion area (1.77 cm<sup>2</sup>),  $P_{app}$  is the apparent permeability, and  $C_d$  is the total CBZ/CD concentration in the donor phase.

To assure sink conditions, common guidelines were followed, where both volume change and final concentration of components in donor phases were assessed.<sup>35,38</sup>

The calculation of the apparent cac for 3.5–5 kDa (i.e., concentration from where aggregates size starts to be larger than the studied pore size, leading to a deviation of ideal flux of CDs through the membrane) was performed by drawing tangent lines in the flux graphics (starting at low concentrations). The deviation point from where the flux started to divert from linearity corresponded to apparent cac value.<sup>34</sup>

## ■ ASSOCIATED CONTENT

### 📄 Supporting Information

The Supporting Information is available free of charge on the ACS Publications website at DOI: 10.1021/acsomega.8b02045.

Analysis of the solid CBZ/CD complexes by FTIR spectroscopy, DSC, and X-ray powder diffractometry (XRPD) (PDF)

## ■ AUTHOR INFORMATION

### Corresponding Author

\*E-mail: thorstlo@hi.is (T.L.).

### ORCID

Thorsteinn Loftsson: 0000-0002-9439-1553

### Notes

The authors declare no competing financial interest.

## ■ ACKNOWLEDGMENTS

The financial support received from the Institute for the Promotion of Innovation through Science and Technology in Flanders (IWT) (grant no. 135040) is gratefully acknowledged.

## ■ REFERENCES

- (1) Koester, L. S.; Mayorga, P.; Pereira, V. P.; Petzhold, C. L.; Bassani, V. L. Carbamazepine/ $\beta$ CD/HPMC Solid Dispersions. II. Physical Characterization. *Drug Dev. Ind. Pharm.* **2003**, *29*, 145–154.
- (2) Cvetkovskii, A.; Bettini, R.; Tasic, L.; Stupar, M.; Casini, I.; Rossi, A.; Giordano, F. Thermal Properties of Binary Mixtures of  $\beta$ -Cyclodextrin with Carbamazepine Polymorphs. *J. Therm. Anal. Calorim.* **2002**, *68*, 669–678.
- (3) Koester, L. S.; Xavier, C. R.; Mayorga, P.; Bassani, V. L. Influence of  $\beta$ -cyclodextrin complexation on carbamazepine release from hydroxypropyl methylcellulose matrix tablets. *Eur. J. Pharm. Biopharm.* **2003**, *55*, 85–91.
- (4) Smith, J. S.; MacRae, R. J.; Snowden, M. J. Effect of SBE7- $\beta$ -cyclodextrin complexation on carbamazepine release from sustained release beads. *Eur. J. Pharm. Biopharm.* **2005**, *60*, 73–80.
- (5) Brewster, M. E.; Anderson, W. R.; Meinsma, D.; Moreno, D.; Webb, A. I.; Pablo, L.; Estes, K. S.; Derendorf, H.; Bodor, N.; Sawchuk, R.; Cheung, B.; Pop, E. Intravenous and oral pharmacokinetic evaluation of a 2-hydroxypropyl-beta-cyclodextrin-based formulation of carbamazepine in the dog: comparison with commercially available tablets and suspensions. *J. Pharm. Sci.* **1997**, *86*, 335–339.
- (6) Strachan, C. J.; Howell, S. L.; Rades, T.; Gordon, K. C. A theoretical and spectroscopic study of carbamazepine polymorphs. *J. Raman Spectrosc.* **2004**, *35*, 401–408.
- (7) Czernicki, W.; Baranska, M. Carbamazepine polymorphs: Theoretical and experimental vibrational spectroscopy studies. *Vib. Spectrosc.* **2013**, *65*, 12–23.
- (8) Rustichelli, C.; Gamberini, G.; Ferioli, V.; Gamberini, M. C.; Ficarra, R.; Tommasini, S. Solid-state study of polymorphic drugs: carbamazepine. *J. Pharm. Biomed. Anal.* **2000**, *23*, 41–54.
- (9) Brewster, M. E.; Loftsson, T. Cyclodextrins as pharmaceutical solubilizers. *Adv. Drug Delivery Rev.* **2007**, *59*, 645–666.
- (10) Crini, G. Review: a history of cyclodextrins. *Chem. Rev.* **2014**, *114*, 10940–10975.
- (11) Loftsson, T.; Duchêne, D. Cyclodextrins and their pharmaceutical applications. *Int. J. Pharm.* **2007**, *329*, 1–11.
- (12) Jansook, P.; Ogawa, N.; Loftsson, T. Cyclodextrins: structure, physicochemical properties and pharmaceutical applications. *Int. J. Pharm.* **2018**, *535*, 272–284.
- (13) Brewster, M. E.; Anderson, W. R.; Estes, K. S.; Bodor, N. Development of Aqueous Parenteral Formulations for Carbamazepine

through the Use of Modified Cyclodextrins. *J. Pharm. Sci.* **1991**, *80*, 380–383.

(14) Loftsson, T.; Masson, M.; Brewster, M. E. Self-association of cyclodextrins and cyclodextrin complexes. *J. Pharm. Sci.* **2004**, *93*, 1091–1099.

(15) Saokham, P.; Do, T. T.; Van den Mooter, G.; Loftsson, T. Inclusion complexes of p-hydroxybenzoic acid esters and  $\gamma$ -cyclodextrin. *J. Inclusion Phenom. Macrocyclic Chem.* **2018**, *90*, 111–122.

(16) Sa Couto, A.; Salustio, P.; Cabral-Marques, H. Cyclodextrins (CDs). In *Polysaccharides: Bioactivity and Biotechnology*; Ramawat, K. G., Merillon, J.-M., Eds.; Springer International Publishing: Switzerland, 2015; pp 247–288.

(17) Stappaerts, J.; Do Thi, T.; Dominguez-Vega, E.; Somsen, G. W.; Van den Mooter, G.; Augustijns, P. The impact of guest compounds on cyclodextrin aggregation behavior: A series of structurally related parabens. *Int. J. Pharm.* **2017**, *529*, 442–450.

(18) Ryzhakov, A.; Do Thi, T.; Stappaerts, J.; Bertolletti, L.; Kimpe, K.; Sa Couto, A. R.; Saokham, P.; Van den Mooter, G.; Augustijns, P.; Somsen, G. W.; Kurkov, S.; Inghelbrecht, S.; Arien, A.; Jimidar, M. I.; Schrijnemakers, K.; Loftsson, T. Self-Assembly of Cyclodextrins and Their Complexes in Aqueous Solutions. *J. Pharm. Sci.* **2016**, *105*, 2556–2569.

(19) Medarevic, D.; Kachrimanis, K.; Djuric, Z.; Ibric, S. Influence of hydrophilic polymers on the complexation of carbamazepine with hydroxypropyl- $\beta$ -cyclodextrin. *Eur. J. Pharm. Sci.* **2015**, *78*, 273–285.

(20) Loftsson, T.; Magnusdottir, A.; Masson, M.; Sigurjonsdottir, J. F. Self-association and cyclodextrin solubilization of drugs. *J. Pharm. Sci.* **2002**, *91*, 2307–2316.

(21) Al-Meshal, M. A.; El-Mahrook, G. M.; Al-Angary, A. A.; Gouda, M. K. Interaction of carbamazepine with cyclodextrins. *Pharm. Ind.* **1993**, *55*, 1129–1132.

(22) El-Nahas, S. A. Physico-chemical characteristics of carbamazepine- $\beta$ -cyclodextrin inclusion compounds and carbamazepine-PEG solid dispersions. *Pharmazie* **1996**, *51*, 960–963.

(23) Loftsson, T.; Fridriksdottir, H. The effect of water-soluble polymers on the aqueous solubility and complexing abilities of  $\beta$ -cyclodextrin. *Int. J. Pharm.* **1998**, *163*, 115–121.

(24) Choudhury, S.; Nelson, K. F. Improvement of oral bioavailability of carbamazepine by inclusion in 2-hydroxypropyl- $\beta$ -cyclodextrin. *Int. J. Pharm.* **1992**, *85*, 175–180.

(25) Kou, W.; Cai, C.; Xu, S.; Wang, H.; Liu, J.; Yang, D.; Zhang, T. In vitro and in vivo evaluation of novel immediate release carbamazepine tablets: complexation with hydroxypropyl- $\beta$ -cyclodextrin in the presence of HPMC. *Int. J. Pharm.* **2011**, *409*, 75–80.

(26) Loftsson, T.; Hreinsdottir, D.; Masson, M. Evaluation of cyclodextrin solubilization of drugs. *Int. J. Pharm.* **2005**, *302*, 18–28.

(27) Jain, A. S.; Date, A. A.; Pissurlenkar, R. R. S.; Coutinho, E. C.; Nagarsenker, M. S. Sulfobutyl Ether- $\beta$ -Cyclodextrin (SBE $_7$   $\beta$ -CD) Carbamazepine Complex: Preparation, Characterization, Molecular Modeling, and Evaluation of In Vivo Anti-epileptic Activity. *AAPS PharmSciTech* **2011**, *12*, 1163–1175.

(28) Coleman, A. W.; Nicolis, I.; Keller, N.; Dalbiez, J. P. Aggregation of cyclodextrins: An explanation of the abnormal solubility of  $\beta$ -cyclodextrin. *J. Inclusion Phenom. Mol. Recognit. Chem.* **1992**, *13*, 139–143.

(29) Wu, A.; Shen, X.; He, Y. Investigation on gamma-cyclodextrin nanotube induced by N,N'-diphenylbenzidine molecule. *J. Colloid Interface Sci.* **2006**, *297*, 525–533.

(30) Higuchi, T.; Connors, K. A. Phase-solubility techniques. In *Advances in Analytical Chemistry Instrumentation*; Reilly, C., Ed.; Wiley-Interscience: New York, 1965; Vol. 4; pp 117–212.

(31) Pitha, J.; Milecki, J.; Fales, H.; Pannell, L.; Uekama, K. Hydroxypropyl- $\beta$ -cyclodextrin: preparation and characterization; effects on solubility of drugs. *Int. J. Pharm.* **1986**, *29*, 73–82.

(32) Loftsson, T.; Brewster, M. E. Pharmaceutical applications of cyclodextrins. I. Drug solubilization and stabilization. *J. Pharm. Sci.* **1996**, *85*, 1017–1025.

(33) Hoshino, T.; Uekama, K.; Pitha, J. Increase in temperature enhances solubility of drugs in aqueous solutions of hydroxypropylcyclodextrins. *Int. J. Pharm.* **1993**, *98*, 239–242.

(34) Sa Couto, A. R.; Ryzhakov, A.; Loftsson, T. Self-Assembly of  $\alpha$ -Cyclodextrin and  $\beta$ -Cyclodextrin: Identification and Development of Analytical Techniques. *J. Pharm. Sci.* **2018**, *107*, 2208–2215.

(35) Martin, A. Diffusion and Dissolution. In *Physical Pharmacy*, 4th ed.; Martin, A., Ed.; Lea & Febiger: Philadelphia, 1993; pp 324–361.

(36) Sa Couto, A.; Ryzhakov, A.; Loftsson, T. 2-Hydroxypropyl- $\beta$ -cyclodextrin aggregates: Identification and development of analytical techniques. *Materials* **2018**, *11*, 1971.

(37) Jansook, P.; Moya-Ortega, M. D.; Loftsson, T. Effect of self-aggregation of  $\gamma$ -cyclodextrin on drug solubilization. *J. Inclusion Phenom. Macrocyclic Chem.* **2010**, *68*, 229–236.

(38) Brodin, B.; Steffansen, B.; Nielsen, C. U. Passive diffusion of drug substances: the concepts of flux and permeability. In *Molecular Biopharmaceutics: Aspects of Drug Characterisation, Drug Delivery and Dosage Form Evaluation*; Steffansen, B., Birger Brodin, B., Carsten Uhd Nielsen, C. U., Eds.; PharmaPress Ltd., 2010; pp 135–151.

(39) Loftsson, T.; Jarho, P.; Masson, M.; Jarvinen, T. Cyclodextrins in drug delivery. *Expert Opin. Drug Delivery* **2005**, *2*, 335–351.